SPATIAL LIGHT MODULATION VIA ENHANCED DIFFRACTION EFFICIENCY OF PHOTOCHROMIC GRATINGS IN PHOTOREFRACTIVE BSO

S.L. Clapham and R.W. Eason

Department of Physics,

The University,

Highfield,

Southampton,

SO9 5NH

U.K.

N.A. Vainos

SERC - Central Laser Facility

Rutherford Appleton Laboratory,

Chilton,

Didcot,

Oxfordshire,

OX11 0QX

U.K.

Abstract

We report a novel scheme for spatial light modulation in which the diffraction efficiency of a permanent photochromic hologram stored in photorefractive BSO is spatially enhanced by illumination with a laser beam at the strongly absorbed blue wavelength, λ = 488 nm. Experimental results and characteristics of this enhancement process are presented, and possible causes discussed.

Bismuth silicon oxide (BSO) is a crystalline material that has been used extensively in the fields of real-time holography and optical image processing [1,2]. In a previous paper [3] we presented a technique for storing holograms in BSO that combines reversible photochromic effects with the more usual real-time photorefractive characteristics. Photochromic effects have been observed before in these sillenite crystals [4] but have generally been considered as a problem as far as photorefraction is concerned, due to the increased absorption. The normal photorefractive (PR) behaviour is unaffected, however, and simultaneous multiplexing of both photorefractive (real-time) and photochromic (permanent) holograms is possible in the same crystal volume.

Using this novel scheme, we have demonstrated a number of techniques ranging from image synthesis to holographic interferometry [5]. These are mostly based on the inherently separate nature of these two holographic gratings which can lead to relative phase shifts between the two simultaneously scattered fields by shifting the real-time grating with respect to the permanent one, using optical techniques. Furthermore, the permanent holograms also show unexpected dynamic behaviour in which a fast increase in diffraction efficiency is observed upon illumination by a beam at the Ar^+ ion wavelength λ = 488 nm, which is strongly absorbed (α = 3-10 cm^{-1}). In this letter, we describe some preliminary results of this behaviour, and we present, for the first time, its application to spatial light modulation.

There is a considerable interest in spatial light modulators (S.L.M's) for use in real-time holography and optical information processing. An SLM is a real-time, reusable device which can produce a coherent optical wavefront that is proportional to the spatial information with which it is optically (or electronically) addressed. Several types of SLM have been investigated in recent years which combine the photosensitivity and electro-optic effects of photorefractive materials. These include the PROM (Pockels readout optical modulator) [6] and a liquid crystal device (LCLV) which uses a single crystal of BSO as the photoconductor in conjunction with a twisted nematic liquid crystal [7-10]. In addition, SLM's based on the modification of gratings can function as combined modulator-holographic element systems, such as the PICOC device [11-13] developed to perform incoherent-to-coherent conversion (ITCC) in a photorefractive four-wave mixing configured BSO crystal.

In our present work real-time and permanent holograms were recorded in BSO and BGO (bismuth germanium oxide) [3]. The holograms were recorded using a multilongitudinal mode argon ion laser, operating at λ = 488 nm, at typical irradiances for the writing beams 1 and 3 of $I_1 = I_3 \simeq 1\text{-}2W\ cm^{-2}$. To investigate the formation of the permanent holograms, recording was performed at several Bragg angles ($\theta = 1^o - 15^o$) and the combined diffraction efficiency (η_T) of the real-time and permanent gratings was monitored by using a Bragg matched He-Ne beam 2 at λ = 633 nm (~5 mW). Hologram exposure times were in the range of 5 minutes to more than 300 minutes, depending on which crystals were used.

Fig.1 shows a typical recording representing the temporal development of holograms for a Bragg angle of $\theta=1.25^{o}$. Curve (a) shows the total diffraction efficiency, η_T, of the combination of real-time and permanent gratings recorded simultaneously in the same crystal volume. Curve (c) depicts the diffraction efficiency of the permanent hologram alone, η_p. This was achieved by periodically blocking the writing beams and sampling the permanent hologram for a period of ~4 seconds. A steady increase in the difference of diffraction efficiencies between permanent, (c), and real-time/permanent, (a), is observed. A significant unexpected effect is observed after the complete erasure of the real-time grating. The diffraction efficiency of the permanent hologram is increased upon illumination by only one of the writing beams at λ=488nm, curve (b). The same effect is also observed when any other intense beam in the green-blue spectral region is used.

The experimental arrangement used to investigate this diffraction efficiency enhancement effect is shown in fig.2. A permanent hologram was recorded in the BSO crystal as described above. The crystal was illuminated with an additional beam 5 at λ = 488 nm at an arbitrary angle. This beam was enlarged using a x4 beam expander to ensure uniform illumination over the entire permanent hologram area. The diffracted readout beam 4 was monitored by a calibrated power meter, D, (Newport model 835) and y-t chart recorder.

Fig.3(a) shows an experimental plot of the diffraction efficiency increase of a permanent hologram recorded in BSO as a function of the irradiance of the blue (λ=488nm) enhancing beam [3]. We have observed that only ~ 2mW cm^{-2} is enough to produce a six-fold increase in the diffraction efficiency, η_p. Fig.3(b) is a schematic diagram showing typical characteristic curves of diffraction efficiency enhancement versus the irradiance of the enhancing beam at λ = 488 nm. Such curves were obtained on varying such experimental parameters as the exposure times, Bragg angles, recording irradiances and crystal orientation. Specifically, we have found that the enhancement factor, or contrast, is critically dependent on the polarisation of the He-Ne readout beam 2 and on the particular crystal orientation used. A maximum contrast ratio of 6:1 was obtained with a BSO crystal oriented for optimum diffraction efficiency [1]. By varying the polarisation of the input He-Ne beam, however, a controllable contrast was obtained that was dependent on both the crystal orientation and from which side of the crystal the Bragg matched He-Ne readout beam was diffracted (see fig.4). Data recorded from these experiments shows a contrast factor that can be easily varied between values of ~1 to ~6.

Regarding the explanation of the observed enhancement behaviour, it is likely that there are secondary photorefractive effects associated with the presence of these photochromic gratings. Such secondary, or parasitic, gratings may be formed due to charge separation generated by photochromic reactions. The parasitic gratings would produce a scattered field which carries a $\pm\pi/2$ phase

shift due to photorefraction [1] and an additional $-\pi/2$ shift due to the scattering process [15]. The role of these parasitic gratings and their dynamic behaviour is the subject of on-going study.

The experimental arrangement in fig. 5 was used to demonstrate spatial light modulation via this irradiance dependent enhancement effect. A permanent hologram, with a characteristic enhancement curve as shown in fig. 3(a), was recorded with a grating spacing, Λ, of 1.6 microns. An object (part of a test chart), placed at position '0' in the enhancing beam 5, was imaged onto the crystal by a x2.5 objective lens, L1 (f = 45 mm, NA = 0.07). The output was monitored by a vidicon camera with the aid of lens L2 (f = 100 mm, f/3). A test chart image, corresponding to those parts of the permanent hologram enhanced by the illuminating object beam, was observed on a T.V. monitor. Fig. 6 shows preliminary results of this spatial enhancement of the permanent hologram. The resolution of the images obtained here is $\sim$ 25 microns. Our value of resolution obtained probably depends on parameters such as the grating spacing, Λ, choice of crystal length, and the nature of the optics used to image the test object onto the crystal (depth of focus). From these considerations, it is possible that a further improvement in resolution is achievable.

The contrast has not been measured for this particular set of results but it is likely that contrast ratios of the order of 6:1 are achievable by this technique, corresponding to the data shown in Fig.3(a).

We have to underline here that the present spatial light modulation scheme is different from the PICOC technique [11-13]. PICOC relies upon the selective modification of a photorefractive grating, resulting in decreased diffraction efficiency and contrast reversal with respect to the input. The present method is based on the selective enhancement of a permanent hologram, in principle yielding the original contrast which is clearly advantageous. The compactness of the device and the submillisecond speed of operation [3] are other advantages.

We are currently investigating the nature of the enhancement process to enable us to improve the quality and resolution of the images. As the enhancement process has a very fast irradiance dependent response time, scanning enhancement of the permanent hologram is also feasible. In addition, there is the possibility of enhancement not by a simple beam, or image, but by a secondary holographic interference pattern. This is an area which is also under current study.

The authors are grateful to the Science and Engineering Research Council and Exitech Ltd., U.K., for a CASE studentship for SLC. Thanks also go to Dr.L. Laycock of GEC Hirst Research Centre, U.K., for supplying a crystal of BSO with known photochromic properties.

REFERENCES

[1] P. Gunter, Phys.Rep., 93, 199 (1982).

[2] R.A. Fisher, ed., "Optical Phase Conjugation", Academic Press New York, (1983).

[3] N.A. Vainos, S.L. Clapham, R.W. Eason, in press, Appl.Opt.(1989)

[4] W. Wardzynski, T. Lukasiewicz, J. Zmija, Opt. Commun., 30, 203 (1979).

[5] N.A. Vainos, S.L. Clapham, R.W. Eason, submitted to Appl.Opt. (1988).

[6] R.A. Sprague, P. Nisenson, Opt.Eng., 17, 256 (1978).

[7] P. Aubourg, J.P. Huignard, M. Hareng, R.A. Mullen, Appl.Opt., 21, 3706 (1982).

[8] S.S. Makh, A.D. Hart, P.M. Openshaw, W.L. Baillie, IEE Proc., 133 J , 60 (1986).

[9] W.L. Baillie, P.M. Openshaw, A.D. Hart, S.S. Makh, IEE Proc., 133 J, 65 (1986).

[10] W.L. Baillie, IEE Proc., 134 J, 326 (1987).

[11] Y. Shi, D. Psaltis, A. Marrakchi, A.R. Tanguay,Jr., Appl.Opt., 22, 3665 (1983).

[12] D. Psaltis, J. Yu, A. Marrakchi, A.R. Tanguay,Jr., Proc. SPIE, 465, 1 (1984).

[13] A. Marrakchi, A.R. Tanguay,Jr., J. Yu, D. Psaltis, Opt.Eng., 24, 124 (1985).

[14] L. Laycock, GEC Hirst Research Centre, Wembley, U.K., Private Communication.

[15] H.Kogelnik, Bell Syst. Tech. J., 48, 2909 (1969).

FIGURE CAPTIONS

Fig.1. Temporal development of a permanent hologram. Recorded diffraction efficiency of (a) the combined permanent and real-time holograms, η_T; (b) the permanent hologram in the presence of one of the writing beams, and (c) the permanent hologram only, η_p, as a function of exposure time. (Taken from [3]).

Fig.2. Experimental configuration used to investigate the diffraction efficiency enhancement effect. (x4 B.EXP = x4 beam expander, IF = He-Ne interference filter, D = calibrated power meter connected to the y-t chart recorder).

Fig.3. Diffraction efficiency enhancement effect. 3(a) shows experimental plot of the enhanced diffraction efficiency of the permanent hologram as a function of the irradiance, I_5, of the enhancing beam at λ = 488 nm. The arrow indicates the initial (unenhanced) diffraction efficiency.(Taken from [3]). 3(b) shows schematic diagram of typical characteristic curves of diffraction efficiency enhancement of permanent holograms as a function of the irradiance of the blue enhancing beam, I_5. The arrows indicate two different initial (unenhanced) permanent hologram diffraction efficiencies.

Fig.4. Experimental arrangement for simultaneous enhanced Bragg-matched He-Ne diffraction from either side of the BSO crystal normal.

Fig.5. Experimental configuration used to demonstrate spatial light modulation via the enhancement effect. L1 is a x 2.5 objective lens (F = 45mm, NA = 0.07), L2 is a F = 100mm, F/3 lens.

Fig.6. Results of the spatial enhancement of a permanent hologram. (a) Permanent hologram stored is BSO. (b), (c) Test chart images corresponding to those parts of the hologram enhanced by the illuminating object beam.

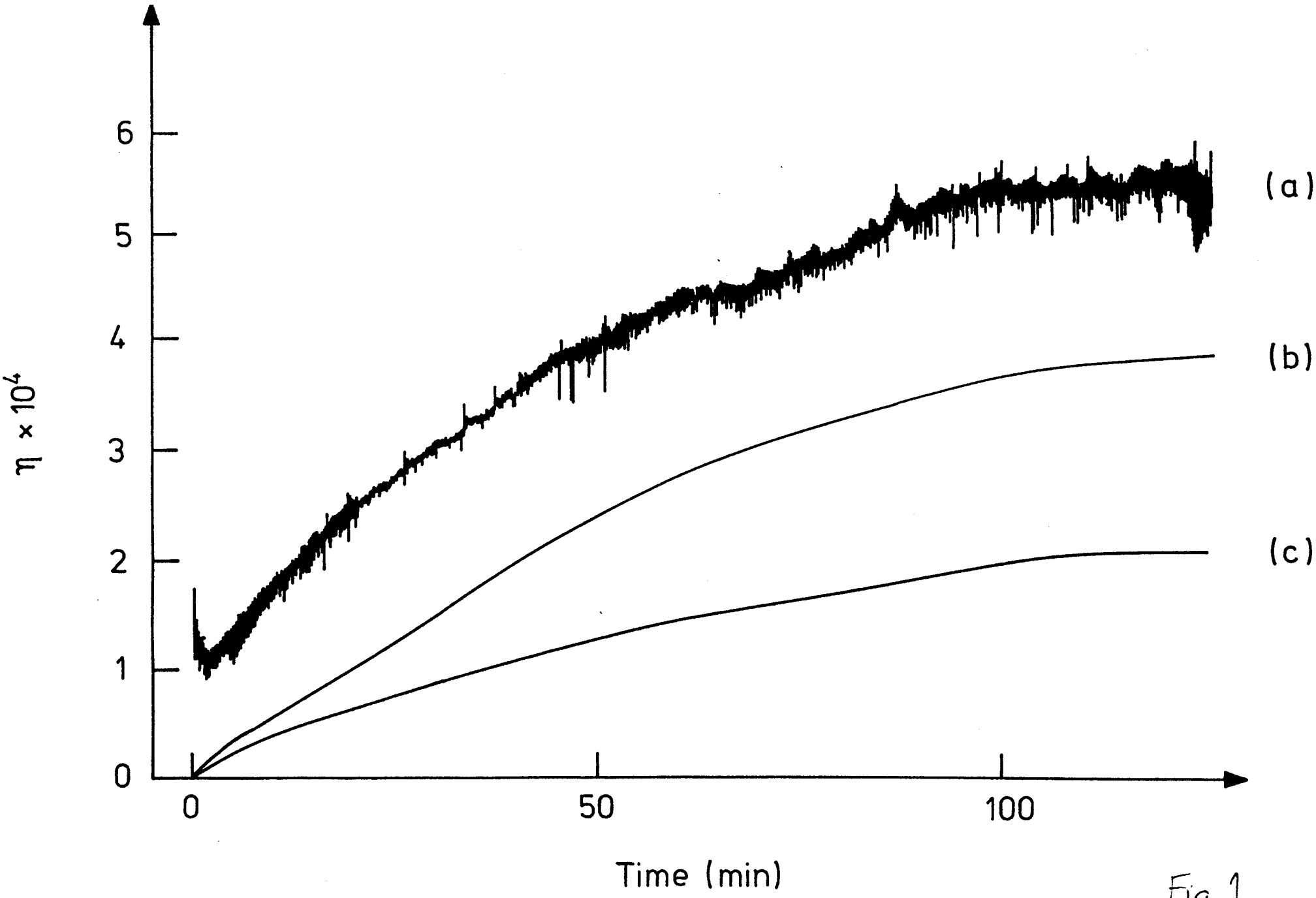

Fig. 1

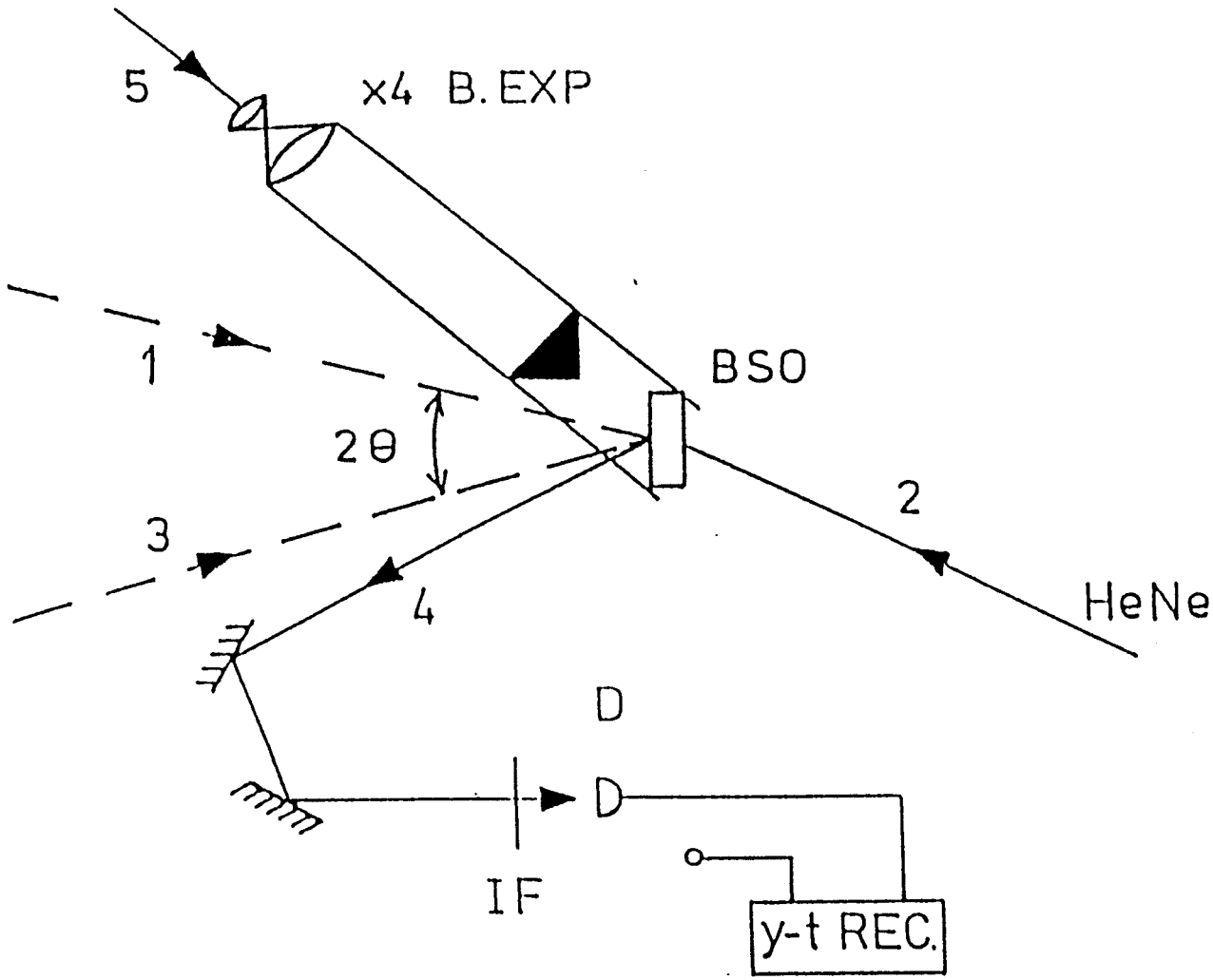

Fig. 2.

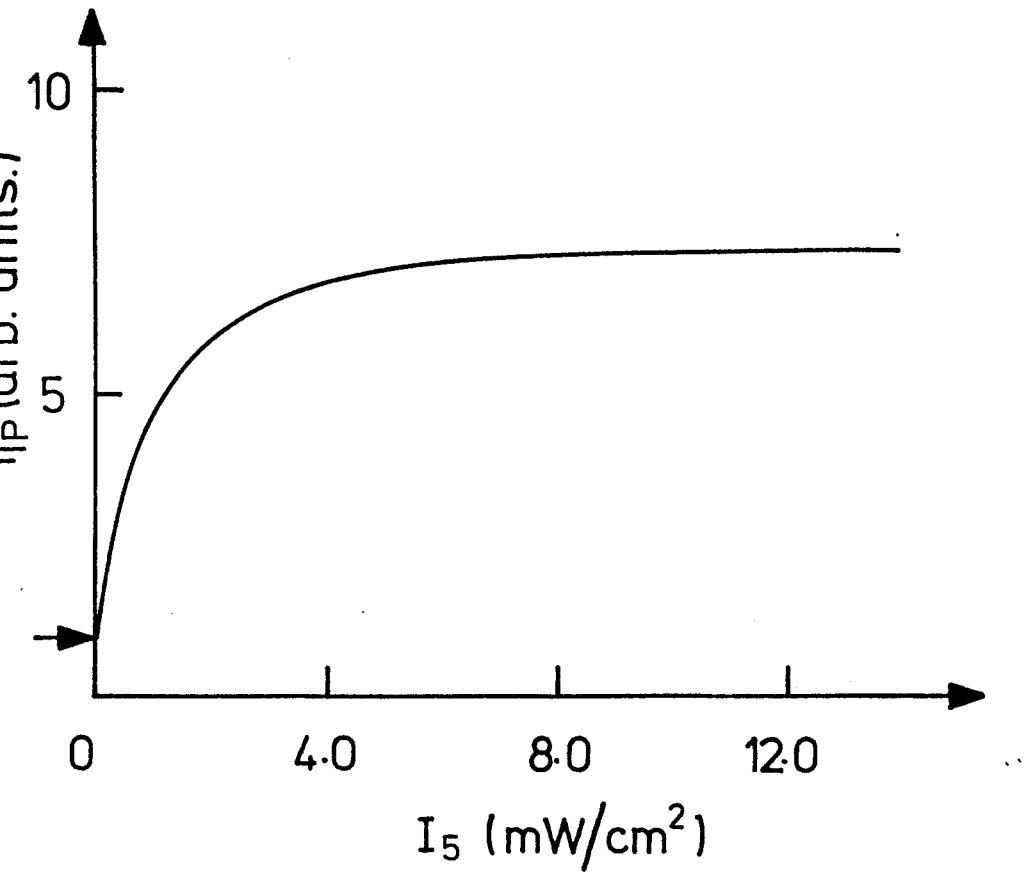

(a)

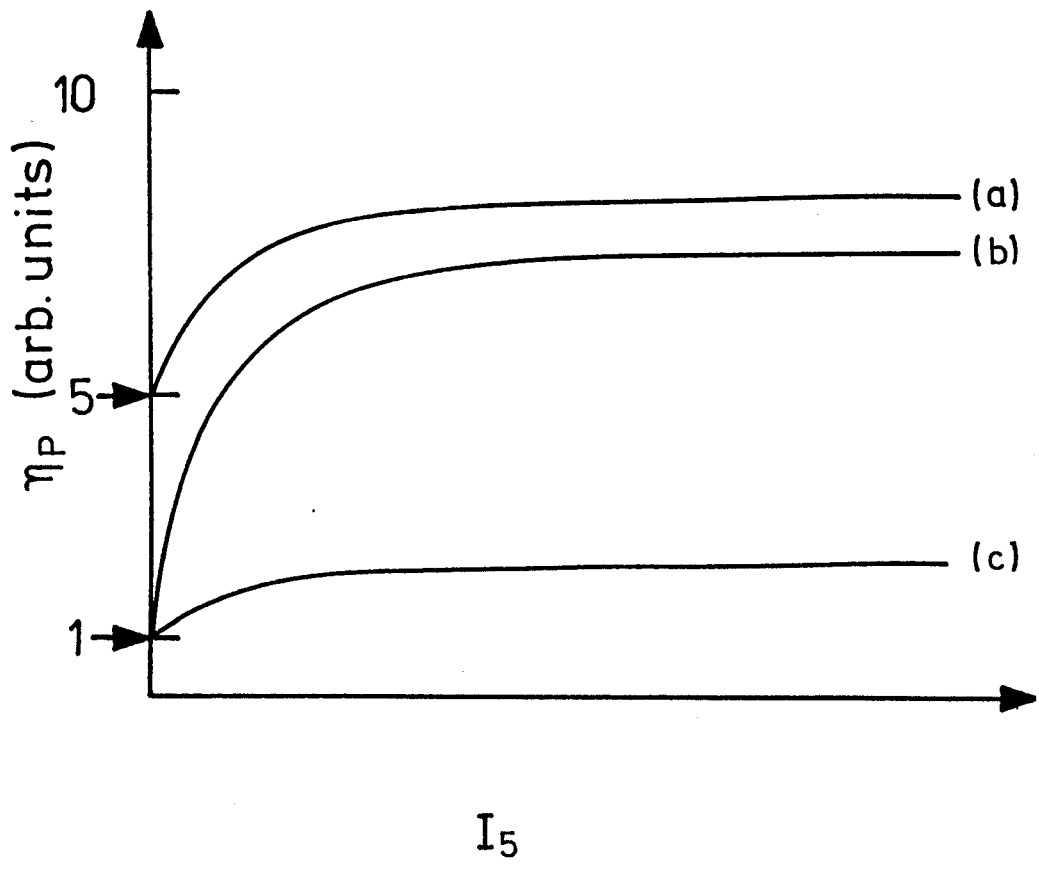

(b)

Fig. 3

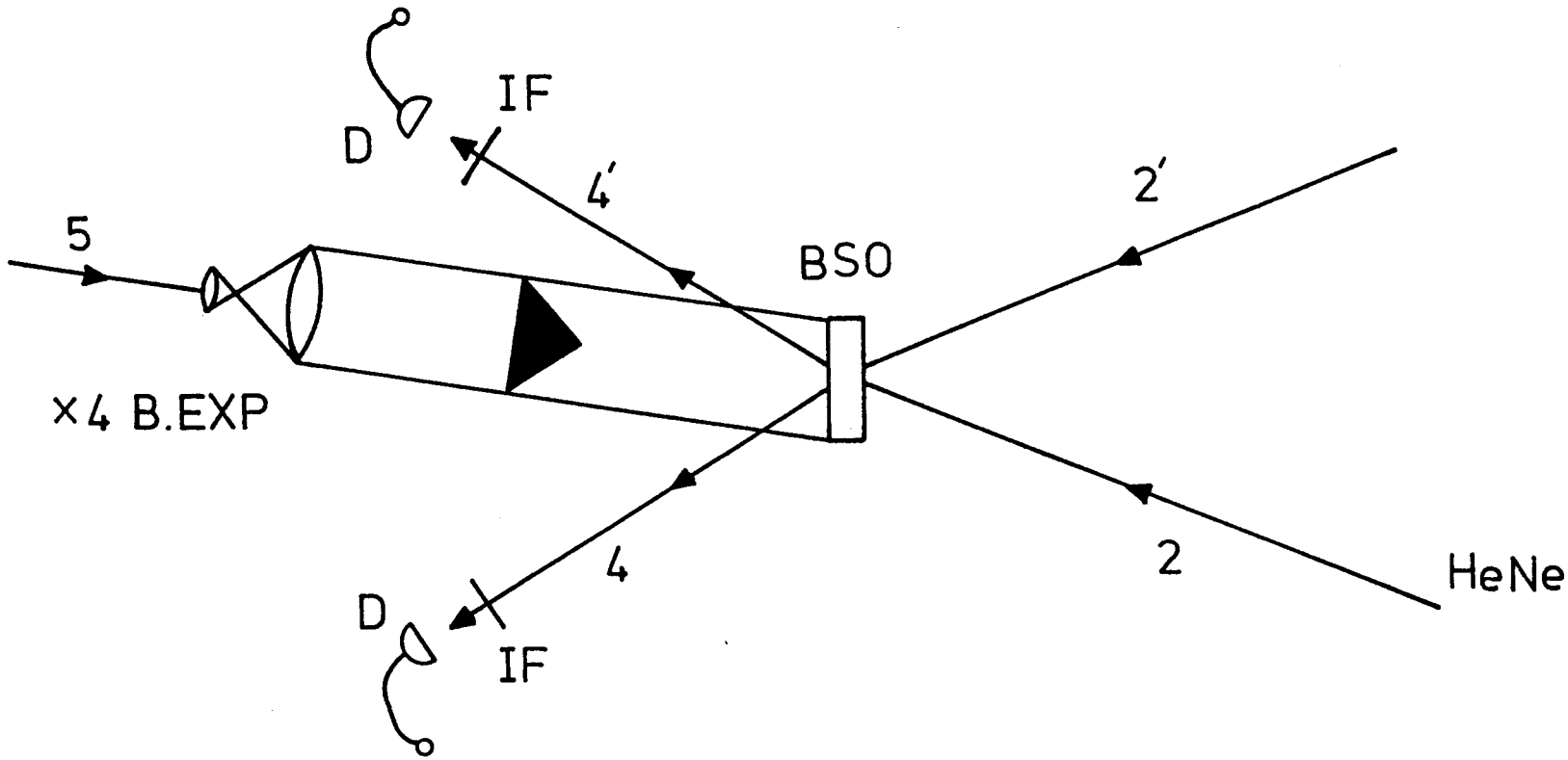

Fig. 4.

Fig.5

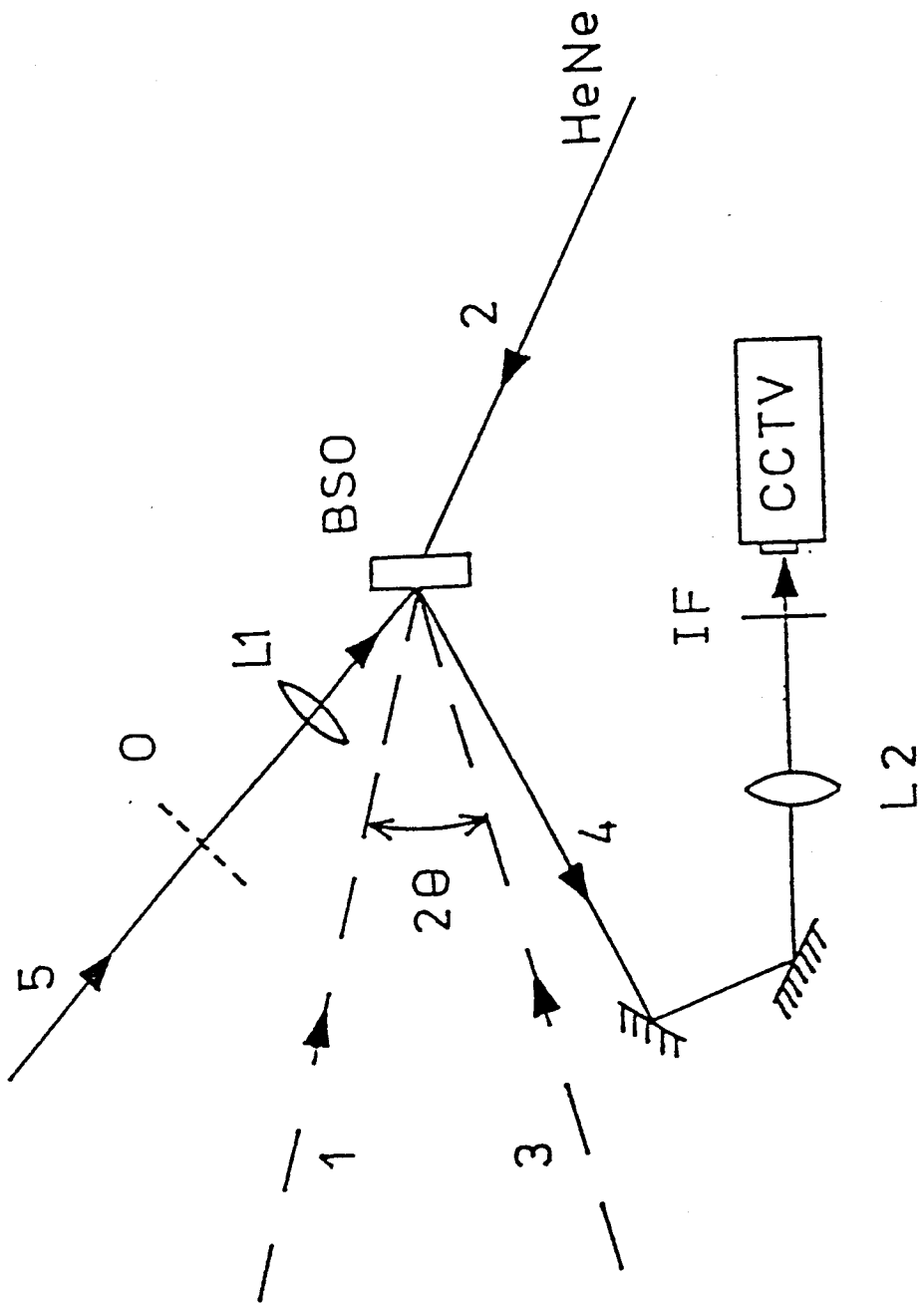

Fig. 6

(a)

(b)

(c)